Direct Strength Method and Response of Cold-Formed Steel Storage Rack Uprights in Global Biaxial Bending

Talebian, Nima; Gilbert, Benoit P.; Miller, Dane; Karampour, Hassan; Habashizadeh, Mohammad Hosein

Ninth International Conference on
THIN-WALLED STRUCTURES – ICTWS2023
Sydney, Australia, Nov 29 – Dec 1, 2023

DIRECT STRENGTH METHOD AND RESPONSE OF COLD-FORMED STEEL STORAGE RACK UPRIGHTS IN GLOBAL BIAXIAL BENDING

N. Talebian[*], B. P. Gilbert[**], D. Miller[*], H. Karampour[**] and M.H. Habashizadeh[***]

* School of Sustainable Development, Faculty of Society and Design, Bond University, Australia
e-mails: ntalebia@bond.edu.au, dmiller@bond.edu.au

** School of Engineering and Built Environment, Griffith University, Australia
e-mails: b.gilbert@griffith.edu.au, h.karampour@griffith.edu.au

*** Department of Civil Engineering, Islamic Azad University- Marand Branch, Iran
e-mail: m_habashi@marandiau.ac.ir

Keywords: Cold-formed steel Racks; Biaxial bending; Global buckling; Direct strength method (DSM).

Abstract. *This study seeks to investigate the global (lateral-torsional) buckling capacity of cold-formed steel (CFS) storage rack uprights under biaxial bending. A previously validated biaxial bending numerical model for local and distortional buckling of CFS rack uprights is used for global buckling. Biaxial bending response of nine unperforated upright cross-sections, each with nine different biaxial bending configurations, were considered. The findings demonstrate that the biaxial bending of the investigated uprights is governed by a nonlinear interaction behavior. DSM predictions including the classical method and the use of inelastic reserve capacity are compared to numerical capacities. The use of the DSM with inelastic reserve capacity as in the AISI-S100 and AS/NZS 4600, results in an overall 3% improvement of the predictions when compared with the classical DSM. A new extended range of the inelastic reserve capacity for global buckling is proposed. When compared with the classical DSM approach, the new extended range results in 14% improvement of the DSM predictions.*

1 INTRODUCTION

In clad-racks, also known as rack-supported buildings, the racking is integrated into the building enclosure, making the buildings more cost-effective but with more complicated structural systems. The structural behaviour of these systems and their constituent parts must be more thoroughly examined to create safe and cost-effective design standards. The uprights, or vertical members, in these structures experience biaxial bending as a result of combined effects of the wind and the vertical loads of the stored items [1, 2]. These uprights are often perforated monosymmetric cold-formed steel (CFS) open sections. Contrary to the current CFS structural design specifications [3-5], which consider a linear interaction equation to design members in biaxial bending, several numerical and experimental studies have reported that the linear equation is conservative and a nonlinear relationship governs the biaxial bending response of cold-formed steel members [1, 2, 6–10].

The local and distortional biaxial bending behaviour of perforated and unperforated CFS storage rack uprights was recently studied by Talebian et al. [1-2]. In order to assess the accuracy of the linear biaxial bending design equation and different forms of the Direct Strength Method (DSM) predictions, parametric experiments on unperforated cross-sections were carried out. The findings showed that the conservative linear interaction equation underestimates the biaxial bending capacity by up to 39% and 46% for local and distortional buckling, respectively. However, global buckling was not evaluated.

The primary goal of this study is to run numerical parametric analyses to capture the global (lateral-torsional) biaxial bending behaviour of CFS storage uprights. This study uses the validated biaxial bending Finite Element (FE) model for local and distortional buckling of CFS rack uprights in [1] to run global biaxial bending analyses. The global biaxial bending responses and capacities of unperforated uprights with a wide range of slenderness values are then determined. Analyses are performed for nine biaxial bending configurations for each of the nine different cross-section types. The report discusses and presents the biaxial bending responses of all uprights under investigation. The DSM accuracy for the global biaxial bending strength of storage rack uprights is also evaluated by comparing DSM predictions with the numerical failure moments obtained from the parametric analysis. These approaches consist of (i) the classical DSM equations given in AISI-S100 [3] and AS/NZS 4600 [4], (ii) considering the inelastic reserve capacity for compact cross-sections, as permitted in the AISI-S100 [3] and AS/NZS 4600 [4], and (iii) using a new extended range of the cross-sectional slenderness for the inelastic reserve capacity in global buckling, similar to the one proposed by Pham and Hancock [11] for local and distortional buckling.

2 BIAXIAL BENDING FINITE-ELEMENT MODEL FOR GLOBAL BUCKLING

78 tests on short (local buckling mode) and medium length (distortional buckling mode) perforated and unperforated storage rack uprights under biaxial bending were conducted by Talebian et al. in [2]. Two types of storage rack upright cross-sections, one semi-compact cross-section and one compact cross-section, were tested. To connect to the test rig and prevent warping, steel plates were welded to the ends of the uprights on both sides. For each type of upright, seven alternative biaxial bending configurations were evaluated in order to determine the ultimate failure moments. At the midpoint of each specimen's length, cross-sectional deformations were measured.

The numerical modelling of cold-formed steel members has been well-established in the literature [14], and the FE model used in this work follows the recommendations in [12-17]. Using the software ABAQUS [18], the non-linear biaxial bending responses of the uprights investigated in [2] for local and distortional buckling were numerically reconstructed in [1]. The FE model created for local and distortional buckling is adapted herein to assess the biaxial bending response of steel storage rack uprights in global buckling.

Four-node S4R shell elements were used to model the uprights and their end plates. Convergence studies were performed on all uprights in bending about major axis and an element size of 3 mm x 3 mm was determined to be suitable. For all upright portions in all configurations, this mesh size was employed [19]. Warping was restrained using plates that were rigidly attached to the ends of the uprights, similar to the experimental tests [1-2, 20]. To replicate the simply supported test setup and maintain a constant bending moment along the length of the uprights, a concentrated biaxial bending moment was applied at the locations of the upright's centroidal axis, at both ends of the upright.

The von Mises yield criterion and isotropic hardening were used to consider material nonlinearity in the specimens. The material parameters of the flat portions of the cross sections were determined using a multilinear stress-strain relationship, with nominal properties (Young's modulus of 200 GPa and a yield stress of 450 MPa) used in [1] when doing parametric analyses. For the corner zones of the upright sections with increased yield strength, elastic-perfectly plastic behaviour was assumed and determined by the equations provided in [21]. These equations were derived from coupon tests and therefore consider the residual stress. True stress and strain were employed in the numerical model.

When the upright was subjected to the biaxial bending moment, pure global geometric imperfections were added to the perfect mesh by using the first global elastic buckling mode.

The scale factor for the deformed shapes caused by elastic buckling was L/1000 [22-23], where L is the upright's length. The Modified Riks method was selected to perform geometric and material nonlinear analyses [18]. The analyses were run statically to determine the peak failure moment. The FE model and boundary conditions for a typical upright are shown in Figure 1. As depicted in Figure 1, the upright was rotated by an angle α around its centroidal axis while a moment was applied about the global Y-axis to apply a biaxial bending moment.

3 PARAMETRIC STUDIES IN GLOBAL BIAXIAL BENDING

To fully capture the biaxial bending behaviour of CFS storage rack uprights in global buckling, parametric analyses were carried out over a wide variety of cross-sectional shapes and slenderness values, similar to local and distortional buckling in [1]. Slender, semi-compact and compact unperforated upright cross-sections were considered.

The same uprights from [1] were used to investigate nine cross-sectional shapes. Per upright type, nine distinct biaxial bending configurations were examined. In reference to the local y-axis of symmetry and minor x-axis, these included pure bending about the local y-axis (Conf 0), $M_y = 2.5M_x$ (Conf 1), $M_y = M_x$ (Conf 2), $M_x = 2.5M_y$ (Conf 3), bending about the minor x-axis when the lip stiffeners are in compression (Conf 4), $M_y = -2.5M_x$ (Conf 5), $M_y = -M_x$ (Conf 6), $M_x = -2.5M_y$ (Conf 7), and bending about the minor x-axis when the web are in compression (Conf 8), where M_y and M_x are the moments applied about the y- and x-axes, respectively. M_x positive signifies that lip is in compression.

Figure 2 depicts the upright cross-sectional shapes. The Types G and I were taken from the literature. The cross-sectional shapes encountered in the industry, Types C, D, E, F, M, and O, were taken into consideration here with two distinct thicknesses. Table 1 lists the primary cross-sectional dimensions and properties of all upright types.

Based on the "signature curves" from the elastic buckling analyses performed in ABAQUS [18] on the simply supported and warping restrained model, the length of the uprights in the numerical model was determined. For each type, the length of the upright was kept the same for all nine investigated biaxial bending configurations. The lengths were chosen so that no interactive buckling modes would occur. The elastic local buckling moment was sufficiently greater than the global buckling moment for all sections and configurations [24, 25]. The lengths of the uprights were initially chosen, in the distortional-global interaction mode, to have a global-to-distortional elastic buckling moment ratio (R_{GD}) of less than 0.85 for all sections and configurations [24]. Examples of the critical elastic buckling moment (M_{cr}) vs. L curves are shown in Figure 3, together with the critical global buckling mode (M_{crG}) for the chosen buckling length, for Type M uprights with 1.8 mm of thickness in Confs 0 (major axis), 4 and 8 (minor axis). As can be noted, Conf 8, which is the bending about the minor x axis while the web is in compression, governs the length of the upright to be 3500 mm, preventing interactive buckling failure modes from occuring in all investigated configurations. Table 1 also gives the lengths of all uprights.

4 GLOBAL BIAXIAL BENDING RESPONSE AND INTERACTIVE BEHAVIOUR

For all investigated upright, elastic or inelastic global buckling failure mechanisms were observed. Table 2 provides a summary of the normalized ultimate biaxial moment capacities (M_x/M_{bx} and M_y/M_{by}) for all upright types. The numerical bending moment capacities about the x- (minor) and y- (major) axes are assumed to be M_{bx} and M_{by}, respectively. In Table 2, the global buckling slenderness ratio λ_G is:

$$\lambda_G = \sqrt{\frac{M_y}{M_{crG}}} \tag{1}$$

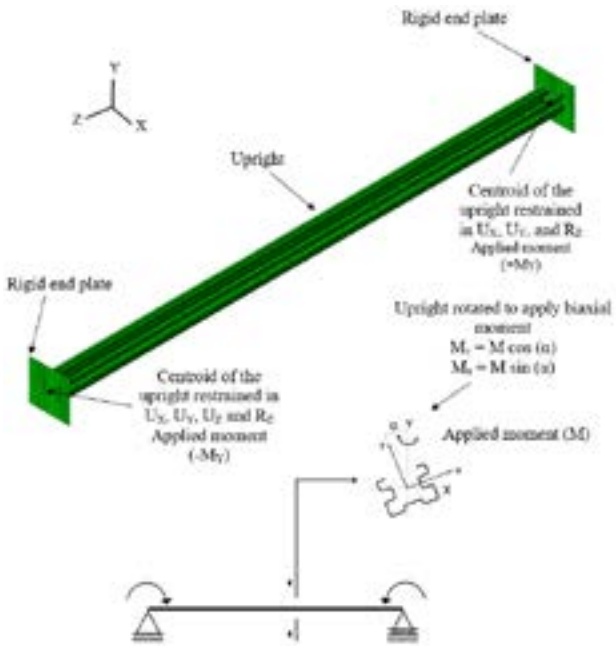

Figure 1: FE model and boundary conditions (shown for Type M upright).

where M_y is the yield biaxial moment and M_{crG} is obtained from the linear buckling analysis (LBA) performed on the FE model. The linear equation currently provided in the standards is used to derive the interactive biaxial moment capacity [3-5]:

$$\frac{M_x}{M_{bx}} + \frac{M_y}{M_{by}} \leq 1.0 \tag{2}$$

The linear design equation versus the normalized biaxial bending results derived from the nine studied configurations are shown in Figure 4. The governing interaction relationship is not linear, as shown in Table 2 and Figure 4.

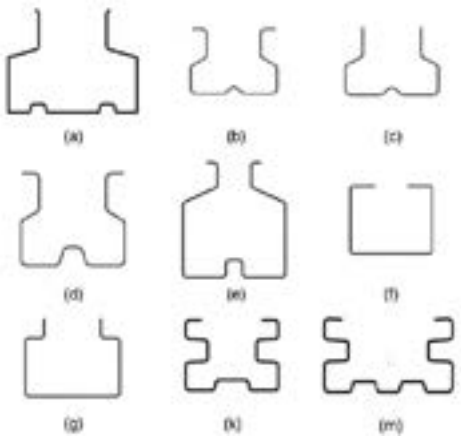

Figure 2: Upright cross sections: (a) Type C; (b) Type D; (c) Type E; (d) Type F; (e) Type G; (f) Type H; (g) Type I (k) Type M; and (m) Type O.

Table 1: Nominal cross-sectional dimensions and properties of investigated uprights in global buckling.

Upright type	Thick. (mm)	Depth (mm)	Width (mm)	I_{major} / I_{minor}	upright length (mm)
Type C	2.0	140	100	2.53	7500
	2.5	140	100	2.53	6800
Type D	1.2	90	72	1.58	5000
	2.0	90	72	1.58	4000
Type E	1.2	90	72	2.06	5000
	2.0	90	72	2.06	4000
Type F	1.5	125	100	1.79	6700
	2.0	125	100	1.79	5500
Type G	2.0	100	110	0.94	8000
Type H	2.5	100	90	1.41	8000
Type I	2.5	100	80	2.13	8000
Type M	1.8	80	60	2.17	3500
	2.5	80	60	2.17	3200
Type O	2.0	120	60	5.05	5500
	2.5	120	60	5.05	5000

With interaction ratios ranging from 0.68 (Type M - Conf 1) to 0.97 (Type D - Conf 1), the linear equation is unconservative for uprights of Type C (Conf 1 and 2), Type D (Conf 1 and 2), Type E (Conf 1 and 3), Type F (Conf 1 and 2), Type H (Conf 1-3), Type I (Conf 1 and 2), Type M (Conf 1), and Type O (Conf 1). The linear equation yields, on average, an unconservative estimate of the biaxial bending capacity of 3% with a coefficient of variation (COV) of 19% for configurations 1 to 3 and for all uprights.

The linear equation is conservative for all upright types when the web is compressed (Conf. 5-7) and yields ratios ranging from 1.21 (Type G - Conf. 5) to 1.45 (Type I - Conf. 6). The linear equation conservatively estimates the biaxial bending capacity by 32%, on average, with a COV of 5% when all uprights and configurations are considered.

Secondary distortional-bifurcation distortional-global interaction (SDI) may occur for sections with $R_{GD} < 1.0$ subject to high yield to non-critical distortional buckling moment ratio (R_y) [24, 25]. The uprights and configurations that exhibit $0.45 < R_{GD} < 0.84$ and $1.03 < R_y < 1.86$ are those where the linear equation is found to be unconservative. According to the analysis of the failure modes for these uprights and configurations, distortional deformations tended to form close to failure, indicating the development of the secondary distortional-bifurcation D-G interaction (SDI) that influences the ultimate strength of the uprights [23]. In Conf 1, Type D uprights with an R_{GD} of 0.56, Type E uprights with an R_{GD} of 0.7, and Type G uprights with an R_{GD} of 0.6 are compared in Figure 5 along with their global and distortional elastic buckling modes and failure modes. In contrast to Type D and E uprights, which experience SDI, Type G uprights collapse in pure global buckling with no indication of distortional deformations, as seen in Figure 5. Performing the analyses for longer uprights, such as the Type E upright (L=12m, $R_{GD} = 0.66$ in Conf 1, $R_{GD} = 0.56$ in Conf 2, and $R_{GD} = 0.55$ in Conf 3), results in the same SDI failure mechanism for these configurations, and the linear biaxial bending design equation is still not conservative. Further investigation is required to assess the impact of cross-sectional shape and dimensions in beams experiencing SDI failure mechanism, The DSM global strength curve can safely manage both the global and SDI failure modes, as will be demonstrated in the next section, eliminating the need to define any border between these two failures.

5 DSM PREDICTIONS

Predicting the biaxial bending capacity of steel storage rack uprights in global buckling using existing DSM-based equations is assessed in this section. The detailed and evaluated approaches are: (i) the classical global DSM equations provided in the AISI-S100 [3] and

AS/NZS 4600 [4], (ii) the global inelastic reserve capacity for stocky cross sections in the AISI-S100 [3] and AS/NZS 4600 [4], and (iii) the newly proposed extended inelastic reserve strength in global buckling.

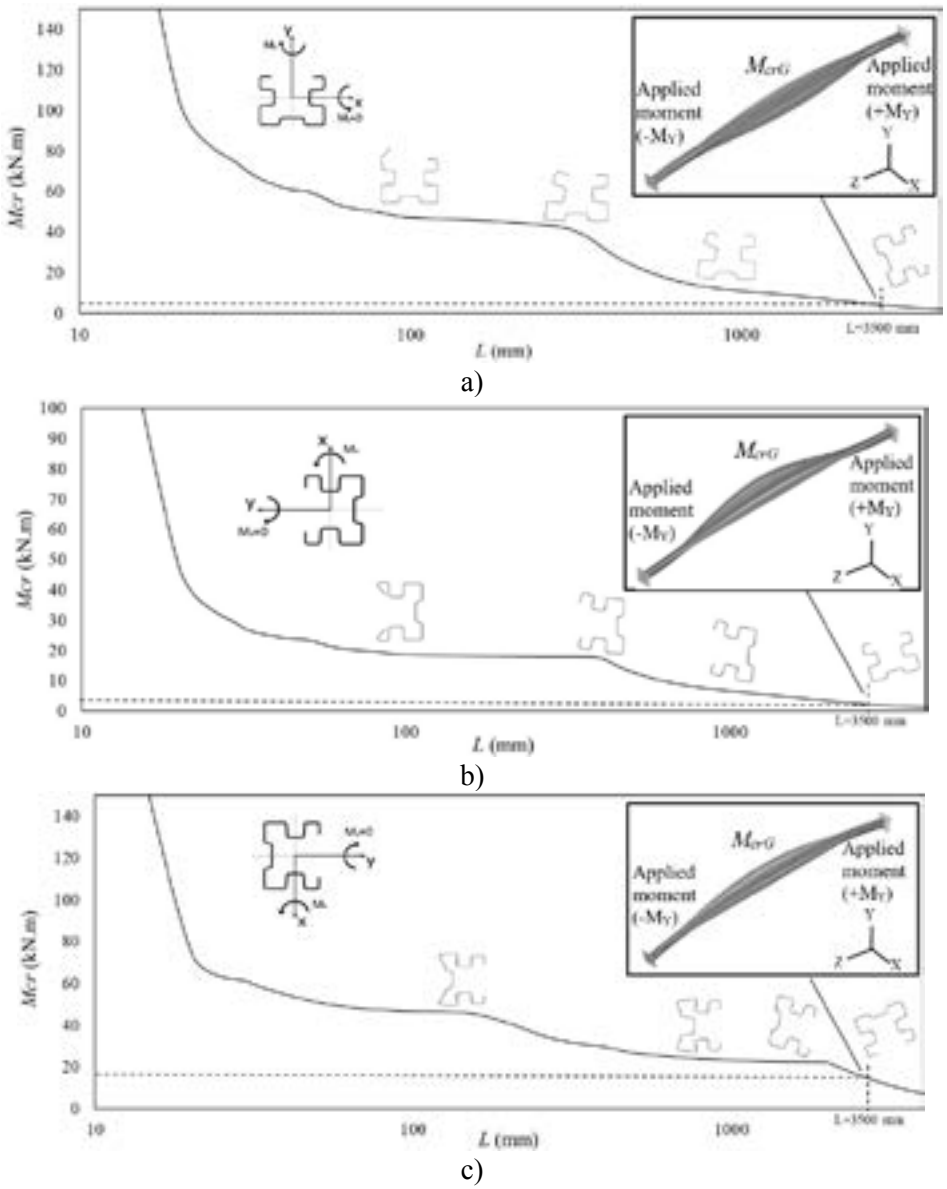

Figure 3: M_{cr} vs. L curves and critical global buckling mode (M_{crG}) of the selected length for 1.8 mm thick Type M upright a) Conf 0 ($M_x = 0$) b) Conf 4 ($M_y = 0$ and lip in compression) c) Conf 8 ($M_y = 0$ and web in compression).

The classical DSM [Approach (i)] nominal member moment capacity, M_{be}, for global buckling, ignoring inelastic reserve capacity, is defined as [3-4, 26-27]

$$M_{be} = M_y \qquad \text{if} \qquad \lambda_G < 0.6 \tag{3}$$

$$M_{be} = \frac{10}{9} M_y \left(1 - \frac{10 M_y}{36 M_{crG}}\right) \qquad \text{if} \qquad 0.6 \le \lambda_G \le 1.336 \tag{4}$$

Table 2: Comparison of parametric studies results with linear equation and DSM for global buckling.

Up-right	Conf.	λ_G	M_y/M_{by}	M_x/M_{bx}	Eq. (2) Linear	DSM M_{FEA}/M_{DSM} (no reserve)[a]	DSM M_{FEA}/M_{DSM} (with reserve)[b]	DSM M_{FEA}/M_{DSM} (extended range)[c]
	0	1.54	1.00	0.00	1.00	1.68	1.68	1.68
	1	1.65	0.45	0.31	0.76	1.12	1.12	1.12
	2	1.38	0.33	0.55	0.88	0.97	0.97	0.97
Type C-2 mm	3	1.15	0.19	0.81	1.00	1.20	1.20	1.15
	4	1.15	0.00	1.00	1.00	1.40	1.40	1.34
	5	1.25	0.97	0.37	1.34	1.42	1.42	1.41
	6	0.92	0.73	0.71	1.44	1.36	1.36	1.23
	7	0.63	0.38	0.93	1.31	1.73	1.73	1.24
	8	0.56	0.00	1.00	1.00	1.80	1.63	1.22
	0	1.37	1.00	0.00	1.00	1.53	1.53	1.53
	1	1.35	0.48	0.31	0.79	0.92	0.92	0.92
	2	1.24	0.34	0.54	0.88	0.95	0.95	0.94
Type C-2.5 mm	3	1.03	0.22	0.86	1.08	1.41	1.41	1.28
	4	1.01	0.00	1.00	1.00	1.58	1.58	1.41
	5	1.12	0.90	0.38	1.28	1.30	1.30	1.26
	6	0.84	0.68	0.72	1.38	1.34	1.34	1.17
	7	0.57	0.36	0.93	1.29	1.79	1.65	1.22
	8	0.50	0.00	1.00	1.00	1.90	1.52	1.22
	0	1.45	1.00	0.00	1.00	1.72	1.72	1.72
	1	1.41	0.43	0.39	0.82	1.07	1.07	1.07
	2	1.45	0.26	0.57	0.83	1.04	1.04	1.04
Type D-1.2 mm	3	1.46	0.15	0.85	1.00	1.31	1.31	1.31
	4	1.63	0.00	1.00	1.00	1.51	1.51	1.51
	5	1.02	0.90	0.33	1.23	1.45	1.45	1.34
	6	0.78	0.71	0.65	1.36	1.55	1.55	1.26
	7	0.64	0.40	0.90	1.30	1.71	1.71	1.27
	8	0.67	0.00	1.00	1.00	1.49	1.49	1.24
	0	1.13	1.00	0.00	1.00	1.42	1.42	1.40
	1	1.13	0.56	0.43	0.99	1.13	1.13	1.09
	2	1.12	0.33	0.65	0.98	1.12	1.12	1.07
Type D-2 mm	3	1.12	0.18	0.86	1.04	1.27	1.27	1.21
	4	1.24	0.00	1.00	1.00	1.33	1.33	1.32
	5	0.83	0.91	0.39	1.30	1.48	1.48	1.28
	6	0.62	0.68	0.72	1.40	1.65	1.65	1.27
	7	0.51	0.35	0.94	1.29	1.81	1.50	1.20
	8	0.53	0.00	1.00	1.00	1.53	1.39	1.16
	0	1.53	1.00	0.00	1.00	1.87	1.87	1.87
	1	1.56	0.38	0.40	0.78	0.95	0.95	0.95
	2	1.43	0.24	0.62	0.86	0.89	0.89	0.89
Type E- 1.2 mm	3	1.28	0.13	0.84	0.97	1.02	1.02	1.02
	4	1.31	0.00	1.00	1.00	1.17	1.17	1.17
	5	1.22	0.92	0.37	1.29	1.43	1.43	1.42
	6	0.88	0.71	0.70	1.41	1.50	1.50	1.31
	7	0.63	0.38	0.93	1.31	1.82	1.82	1.29
	8	0.59	0.00	1.00	1.00	1.80	1.74	1.27
	0	1.19	1.00	0.00	1.00	1.47	1.47	1.46
	1	1.22	0.48	0.36	0.84	0.91	0.91	0.90
	2	1.12	0.31	0.59	0.90	0.97	0.97	0.93
Type E-2 mm	3	1.00	0.17	0.80	0.97	1.23	1.23	1.09
	4	1.01	0.00	1.00	1.00	1.43	1.43	1.29
	5	0.97	0.84	0.39	1.23	1.27	1.27	1.19
	6	0.69	0.63	0.74	1.37	1.47	1.47	1.18
	7	0.50	0.33	0.96	1.29	1.92	1.53	1.21
	8	0.47	0.00	1.00	1.00	1.84	1.42	1.18
	0	1.42	1.00	0.00	1.00	1.53	1.53	1.53
	1	1.42	0.44	0.39	0.83	0.99	0.99	0.99
	2	1.35	0.27	0.60	0.87	0.94	0.94	0.94
Type F-1.5 mm	3	1.34	0.16	0.86	1.02	1.17	1.17	1.17
	4	1.46	0.00	1.00	1.00	1.27	1.27	1.27
	5	1.07	0.87	0.33	1.20	1.33	1.33	1.26
	6	0.75	0.68	0.65	1.33	1.44	1.44	1.16
	7	0.60	0.38	0.90	1.28	1.65	1.65	1.18
	8	0.64	0.00	1.00	1.00	1.47	1.47	1.19
	0	1.19	1.00	0.00	1.00	1.33	1.33	1.31
	1	1.17	0.51	0.39	0.90	0.95	0.95	0.93
	2	1.13	0.34	0.66	1.00	1.05	1.05	1.01
Type F-2 mm	3	1.11	0.18	0.89	1.07	1.23	1.23	1.16
	4	1.22	0.00	1.00	1.00	1.23	1.23	1.21
	5	0.88	0.89	0.36	1.25	1.31	1.31	1.16
	6	0.64	0.68	0.69	1.37	1.53	1.53	1.16
	7	0.51	0.37	0.93	1.30	1.80	1.48	1.18
	8	0.53	0.00	1.00	1.00	1.52	1.37	1.14
	0	1.23	1.00	0.00	1.00	1.40	1.40	1.39
	1	1.27	0.85	0.66	1.51	1.62	1.62	1.61
	2	1.39	0.56	1.10	1.66	1.73	1.73	1.73
Type G-2 mm	3	1.43	0.23	1.10	1.33	1.50	1.50	1.50
	4	1.52	0.00	1.00	1.00	1.32	1.32	1.32
	5	0.99	0.94	0.28	1.22	1.37	1.37	1.27
	6	0.88	0.75	0.55	1.30	1.36	1.36	1.21
	7	0.82	0.44	0.81	1.25	1.57	1.57	1.32
	8	0.84	0.00	1.00	1.00	1.69	1.69	1.46
	0	1.62	1.00	0.00	1.00	2.34	2.34	2.34
	1	1.61	0.35	0.37	0.72	1.16	1.16	1.16
	2	1.64	0.20	0.55	0.75	1.12	1.12	1.12
Type H-2.5 mm	3	1.70	0.12	0.83	0.95	1.47	1.47	1.47
	4	1.90	0.00	1.00	1.00	1.71	1.71	1.71
	5	1.20	0.93	0.36	1.29	1.79	1.79	1.77
	6	0.93	0.71	0.69	1.40	1.71	1.71	1.54
	7	0.80	0.38	0.93	1.31	1.71	1.71	1.46
	8	0.84	0.00	1.00	1.00	1.45	1.45	1.34
	0	1.92	1.00	0.00	1.00	3.07	3.07	3.07
	1	1.88	0.49	0.31	0.80	1.92	1.92	1.92
	2	1.80	0.38	0.59	0.97	2.24	2.24	2.24
Type I-2.5 mm	3	1.59	0.22	0.83	1.05	2.59	2.59	2.59
	4	1.60	0.00	1.00	1.00	2.94	2.94	2.94
	5	1.53	0.93	0.39	1.32	2.39	2.39	2.39
	6	1.15	0.71	0.74	1.45	1.83	1.83	1.78
	7	0.83	0.36	0.94	1.30	1.89	1.89	1.58
	8	0.76	0.00	1.00	1.00	1.81	1.81	1.48
	0	1.39	1.00	0.00	1.00	1.59	1.59	1.59
	1	1.35	0.42	0.26	0.68	0.92	0.92	0.92
	2	1.29	0.43	0.66	1.09	1.50	1.50	1.49
Type M-1.8 mm	3	1.24	0.23	0.89	1.12	1.74	1.74	1.72
	4	1.35	0.00	1.00	1.00	1.83	1.83	1.83
	5	1.02	0.90	0.39	1.28	1.36	1.36	1.27
	6	0.73	0.69	0.74	1.43	1.51	1.51	1.22
	7	0.54	0.35	0.96	1.31	1.72	1.53	1.20
	8	0.54	0.00	1.00	1.00	1.45	1.35	1.14
	0	1.21	1.00	0.00	1.00	1.42	1.42	1.41
	1	1.18	0.48	0.29	0.77	0.95	0.95	0.93
	2	1.12	0.43	0.61	1.04	1.35	1.35	1.30
Type M-2.5 mm	3	1.06	0.23	0.85	1.08	1.66	1.66	1.54
	4	1.15	0.00	1.00	1.00	1.73	1.73	1.69
	5	1.24	0.88	0.42	1.30	1.86	1.86	1.84
	6	0.65	0.67	0.80	1.47	1.59	1.59	1.23
	7	0.49	0.32	0.96	1.28	1.74	1.40	1.15
	8	0.48	0.00	1.00	1.00	1.49	1.28	1.12
	0	2.10	1.00	0.00	1.00	2.35	2.35	2.35
	1	1.96	0.61	0.31	0.92	1.84	1.84	1.84
	2	1.76	0.49	0.62	1.11	2.11	2.11	2.11
Type O-2 mm	3	1.41	0.27	0.85	1.12	2.29	2.29	2.29
	4	1.39	0.00	1.00	1.00	2.50	2.50	2.50
	5	1.56	0.91	0.38	1.29	1.73	1.73	1.73
	6	1.07	0.68	0.72	1.40	1.26	1.26	1.18
	7	0.62	0.36	0.93	1.29	1.53	1.53	1.15
	8	0.49	0.00	1.00	1.00	1.57	1.35	1.15
	0	1.86	1.00	0.00	1.00	1.99	1.99	1.99
	1	1.79	0.62	0.29	0.91	1.57	1.57	1.57
	2	1.54	0.51	0.58	1.09	1.80	1.80	1.80
Type O-2.5 mm	3	1.23	0.29	0.84	1.11	2.05	2.05	2.02
	4	1.21	0.00	1.00	1.00	2.33	2.33	2.29
	5	1.44	0.91	0.41	1.32	1.48	1.48	1.48
	6	0.95	0.68	0.76	1.44	1.23	1.23	1.10
	7	0.55	0.36	0.98	1.34	1.62	1.47	1.14
	8	0.44	0.00	1.00	1.00	1.58	1.25	1.12
		Average (all uprights)			1.10	1.55	1.52	1.41
		COV (%)			18	26	26	29

[a] No inelastic reserve capacity – Approach (i).
[b] Inelastic reserve capacity – Approach (ii).
[c] Newly proposed extended reserve strength in global buckling – Approach (iii).

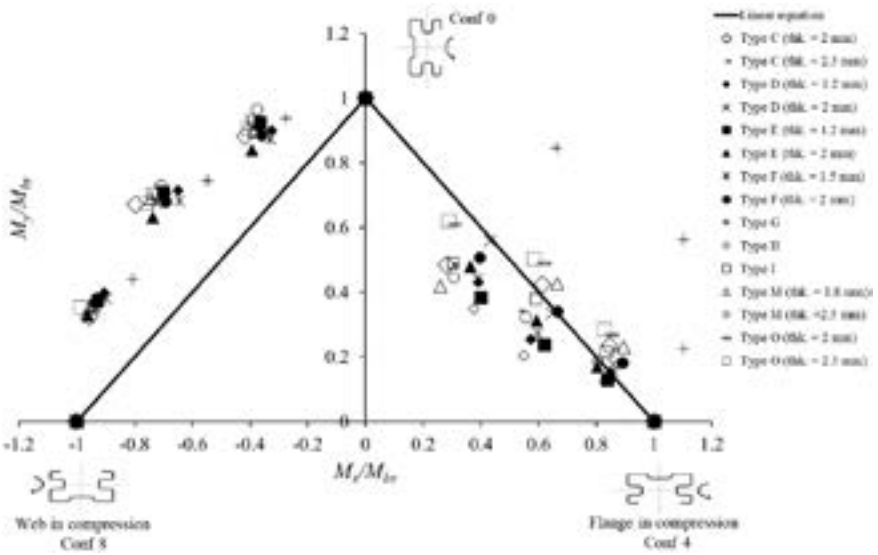

Figure 4: Biaxial bending interaction points for global buckling - all uprights.

$$M_{be} = M_{crG} \qquad \text{if} \qquad \lambda_G > 1.336 \tag{5}$$

where M_{crG} and M_y are elastic global buckling moment and yield moment, respectively, and λ_G is nondimensional slenderness ratio defined by Eq. (1). The recent AISI-S100 [3] and AS/NZS 4600 [4] consider inelastic reserve capacity, allowing the nominal member moment capacity to vary between M_y and the plastic moment M_p for compact cross-sections, i.e., if $\lambda_G < 0.6$. When considering the global inelastic reserve capacity [Approach (ii)], M_{be} becomes:

$$M_{be} = M_p - (M_p - M_y)\left(\frac{\sqrt{\frac{M_y}{M_{crG}}} - 0.23}{0.37}\right) \le M_p \qquad \text{if} \quad \lambda_G < 0.6 \tag{6}$$

The global elastic buckling moments M_{crG} for each tested configuration to be inputted in the DSM expressions were obtained by running LBA. With the yield stress of 450 MPa utilised in the parametric studies, the yield moment (M_y) and plastic moment (M_p) were calculated about the biaxial bending axis for each of the investigated configurations.

A new extended range of the cross-sectional slenderness for which the inelastic strength can be applied [Approach (iii)] is proposed here for global buckling, which is similar to the extended inelastic reserve capacity for local and distortional buckling proposed by Pham and Hancock [11]. The inelastic reserve capacity for global buckling can be expanded and specified as [3, 4, 11]:

$$M_{nyG} = M_y + (1 - 1/C_{yGn}^2)(M_p - M_y) \tag{7}$$

where

$$C_{yGn} = 1 \le \sqrt{1.336/\lambda_G} \le 3 \tag{8}$$

M_{nyG} is then used in the classical DSM [Eqs. (3–5)] instead of M_y, and λ_{Gn} is defined as:

$$\lambda_{Gn} = \sqrt{\frac{M_{nyG}}{M_{crG}}} \tag{9}$$

is used instead of λ_G to obtain the new nominal member capacity with extended range, M_{bGn}.

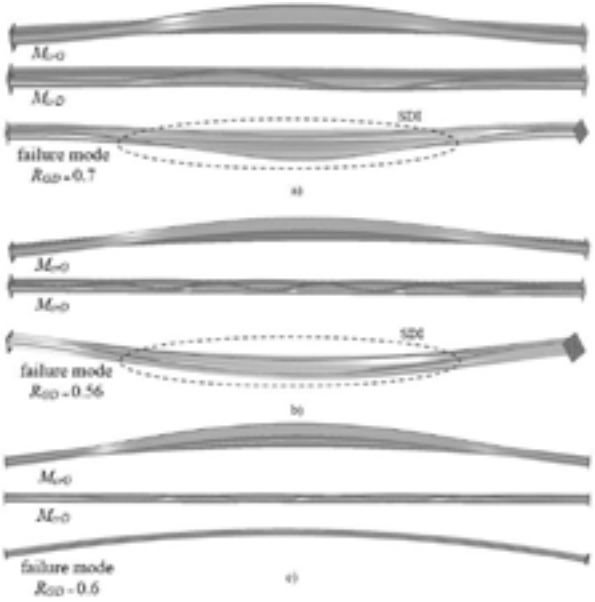

Figure 5: Global buckling (M_{crG}), distortional buckling (M_{crD}), and failure deformed shapes (scale factor =3) in Conf 1 a) Type D upright (thk. = 2 mm) b) Type E upright (thk. = 2 mm) c) Type G upright.

6 COMPARISONS OF DIRECT STRENGTH METHOD WITH PARAMETRIC RESULTS

The ratio of the DSM predicted moment M_{DSM} to the FEA biaxial failure moment M_{FEA} for the three approaches in global buckling is shown in Table 2. The normalized FEA capacities for the conventional DSM [Approach (i)] and the newly proposed extended range [Approach (iii)], for all tested configurations, are graphically compared to the classical DSM global buckling curve in Figure 6. The FEA to DSM capacity ratios range between 0.89 (for 1.2 mm thick Type E - Conf 2) and 3.07 (for Type I - Conf 0), as shown in Figure 6 and Table 2. The classical DSM (without the inelastic reserve capacity) typically results in conservative estimation of the bending capacity of the studied uprights. With a coefficient of variation (COV) of 26% for all evaluated uprights and configurations, the DSM without the inelastic reserve capacity conservatively estimates the bending capacity by 55%.

In the 135 evaluated configurations for the biaxial bending of the nine global buckling sections, 45 configurations have slender cross-sections with a λ_G greater than 1.336, 73 configurations have cross-sections that are between $0.6 \leq \lambda_G \leq 1.336$, and 17 configurations have stocky cross-sections and have a λ_G value lower than 0.6. The standard DSM global strength curve underestimates the capacity by about 64%, with a COV of 34%, when $\lambda_G > 1.336$. In other words, it would be extremely conservative to consider the elastic buckling moment as the failure moment for slender sections.

With an average FEA to DSM biaxial moment capacity of 1.45 and a COV of 18%, the classical DSM provides a conservative prediction of the bending capacity of the examined uprights when $0.6 \leq \lambda_G \leq 1.336$. The classical DSM, with a COV of 9%, typically underestimates the FEA capacity by 70% for stocky sections with $\lambda_G < 0.6$.

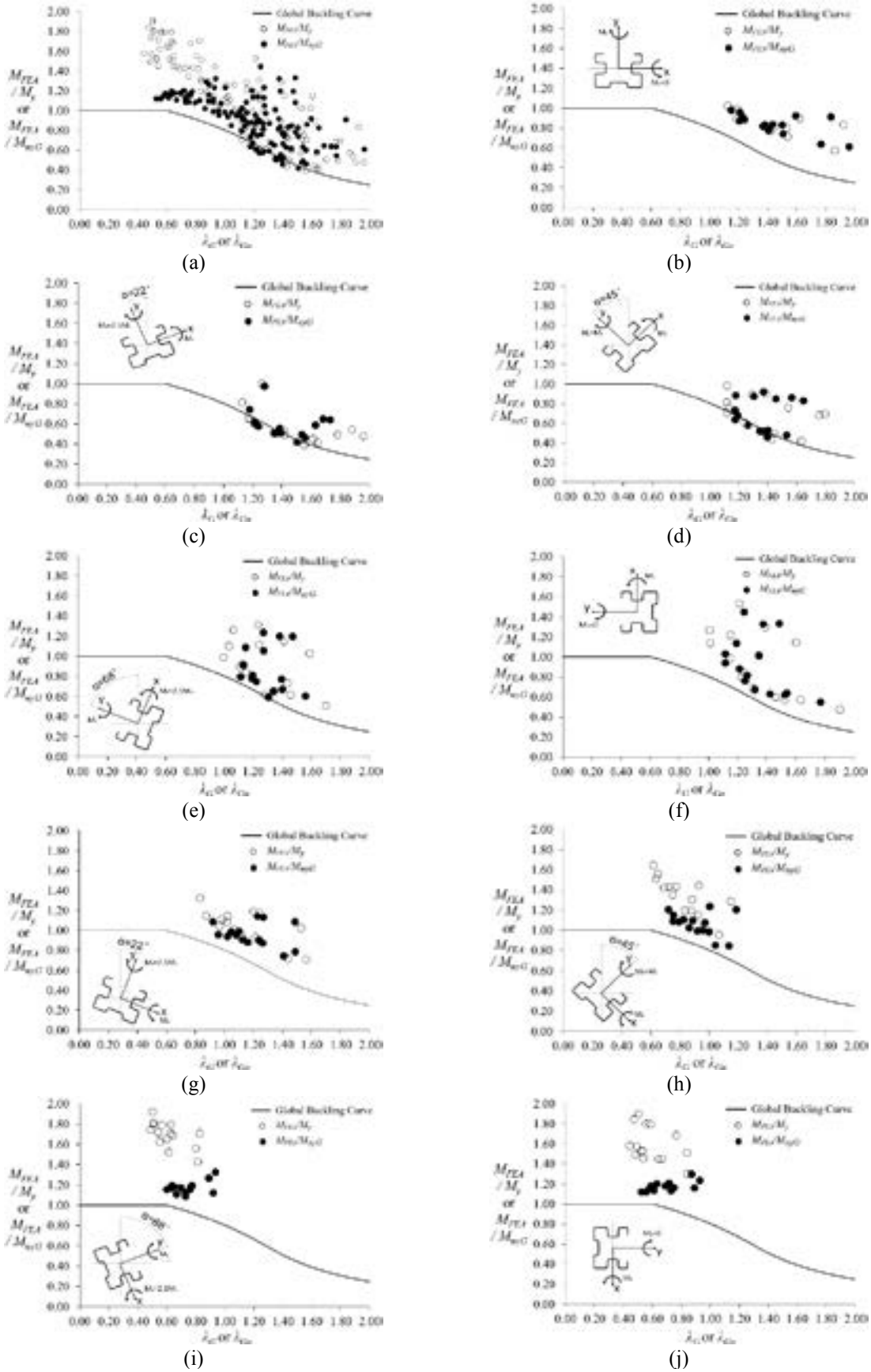

Figure 6: Comparison of the DSM curve to parametric studies data for global buckling [Approach (i) and (iii)] a) all configurations b) Conf 0 (major axis) c) Conf 1 d) Conf 2 e) Conf 3 f) Conf 4 (lip in compression) g) Conf 5 h) Conf 6 i) Conf 7 and j) Conf 8 (web in compression).

Ten out of 15 major configurations (Conf 0) have slender cross sections ($\lambda_G > 1.336$) and fail in elastic buckling at a moment smaller than M_y. Except for one configuration (2mm thick Type D), the rest of the major configurations all fail in elastic buckling with slenderness ratios of $0.6 \leq \lambda_G \leq 1.336$. For bending about the major axis, the average M_{FEA}/M_{DSM} is 1.78. The average M_{FEA}/M_{DSM} for bending about the minor axis (Conf 4 and 8) is 1.66. With an average M_{FEA}/M_{DSM} of 1.35 for Conf 1-3, DSM yields more accurate predictions. For Conf 5-7, DSM results in an average M_{FEA}/M_{DSM} of 1.58.

When compared to the classical DSM, using the DSM with inelastic reserve capacity [Approach (ii)], as in the AISI-S100 [3] and AS/NZS 4600 [4], improves predictions by an average of 3%. Table 2 and Figure 6 show that the proposed method, the new extended range of the inelastic reserve capacity for global buckling [Approach (iii)], provides better strength predictions (primarily for stocky sections) when compared with the previous two DSM approaches. This approach overestimates the FEA capacity, on average, by 41% with a COV of 29%, for all configurations and upright types.

7 CONCLUSIONS

This research presents a numerical analysis of global biaxial bending of cold-formed steel storage rack uprights. To evaluate the accuracy of the linear biaxial bending design equation in the international design codes for global buckling, nine unperforated upright sections were examined. The linear biaxial bending design equation was shown to be conservative, with failure occuring at ratios ranging from 1.00 to 1.47. When the web is in compression, the biaxial bending interaction relationship was found to be nonlinear. Due to the observed secondary-distortion bifurcation D-G interaction, the linear equation is unconservative for some of the examined uprights when the flange is in compression. To estimate the biaxial bending capacity of CFS storage rack uprights failing in global buckling with or without considering the inelastic reserve capacity as specified in design standards, the accuracy of the DSM global strength curve was also evaluated. For all studied configurations, it was discovered that the conventional DSM underestimates the biaxial bending capacity. The ratio of capacity to DSM prediction was, on average, 1.55. This ratio becomes 1.52 when the inelastic reserve capacity is considered. The DSM equations more accurately predicted the biaxial capacity when employing the newly extended range in this study for global inelastic reserve strength, with a capacity to prediction ratio of 1.41.

REFERENCES

[1] Talebian N., Gilbert B. P., Pham C. H., Chariere R., and Karampour H., "Parametric Studies and Design Rules for Local and Distortional Biaxial-Bending Capacity of Cold-Formed Steel Storage-Rack Uprights", *Journal of Structural Engineering*, **146**(3), 04020009, 2020.

[2] Talebian N., Gilbert B. P., Pham C. H., Chariere R., and Karampour H., "Local and distortional biaxial bending capacities of cold-formed steel storage rack uprights, *Journal of Structural Engineering*, **144**(6), 04018062, 2018.

[3] AISI (American Iron and Steel Institute), North American specification for the design of cold-formed steel structural members. AISI-S100, Washington, DC: AISI. 2016.

[4] AS/NZS, Cold-formed steel structures. AS/NZS 4600, Australia: AS/NZS. 2018.

[5] CEN, Eurocode 3. Design of steel structures. General rules. Supplementary rules for cold-formed members and sheeting. EN 1993-1-3, Brussels, Belgium: CEN. 2006.

[6] Put M.B., Pi Y.-L., and Trahair Y.-L., "Lateral buckling tests on cold-formed Z-beams", *Journal of Structural Engineering,* **125**(11), 1277-1283, 1999.

[7] Torabian s., Fratamico D. C., and Schafer B. W., "Experimental response of cold-formed steel zee-section beam-columns", *Thin-walled Structures*, **98**, 496-517, 2016.

[8] Torabian S., Zheng B., and Schafer B.W., "Experimental response of cold-formed steel lipped channel beam-columns", *Thin-walled Structures*, **89**, 152-168, 2015.

[9] Bertoccia L., Comparinia D., Lavacchinib G., Orlandoc M., Salvatoric L., and Spinellic P., "Experimental, numerical, and regulatory P-Mx-My domains for cold-formed perforated steel uprights of pallet-racks", *Thin-walled Structures*. **119**, 151-165, 2017.

[10] Torabian S., and Schafer B. W., "Development and Experimental Validation of the Direct Strength Method for Cold-Formed Steel Beam-Columns", *Journal of Structural Engineering*, **144**(10) 04018175, 2018.

[11] Pham C.H, and Hancock G. J., "Experimental investigation and direct strength design of high-strength, complex C-sections in pure bending", *Journal of Structural Engineering*, **139**(11), 1842-1852, 2013.

[12] Schafer B.W., Lia Z., and Moen C.D., "Computational modelling of cold-formed steel", *Thin-walled Structures,* **48**, 752-762, 2010.

[13] Yua C., and Schafer B. W., "Simulation of cold-formed steel beams in local and distortional buckling with applications to the direct strength method", *Journal of Constructional Steel Research*, **63**(5), 581-590, 2007.

[14] Bernuzzi C., and Simoncelli M., "European design approaches for isolated cold-formed thin-walled beam–columns with mono-symmetric cross-section", *Engineering Structures*, **86**, 225-241, 2015.

[15] Chen M., and Young B., "Experimental and numerical investigation on cold-formed steel semi-oval hollow section compression members", *Journal of Constructional Steel Research*, **151**, 174-184, 2018.

[16] Ye J., Mojtabaei S. M., and Hajirasouliha I., "Local-flexural interactive buckling of standard and optimised cold-formed steel columns", *Journal of Constructional Steel Research*, **144**, 106-118, 2018.

[17] Peiris M., and Mahendran M., "Behaviour of cold-formed steel lipped channel sections subject to eccentric axial compression", *Journal of Constructional Steel Research*, **184**, 106808, 2021.

[18] ABAQUS, Abaqus ver. 6.14 user manual. Providence, RI: ABAQUS. 2015.

[19] Talebian N., Gilbert B. P., Baldassino N., and Karampour H., "Factors contributing to the transverse shear stiffness of bolted cold-formed steel storage rack upright frames with channel bracing members", *Thin-Walled Structures*, **136**, 50-63, 2019.

[20] Rajkannu J. S., and Jayachandran S. A., "Flexural-torsional buckling strength of thin-walled channel sections with warping restraint", *Journal of Constructional Steel Research*, **169,** 106041, 2020.

[21] Karren K.W., "Corner properties of cold-formed steel shapes", *Journal of Structural Engineering*, **93**(1), 401-432, 1967.

[22] AS (Standards Australia), Steel storage racking. AS4084, Sydney, Australia: AS. 2012.

[23] Guimarães V. M., Gilbert B. P., Talebian N., and Wang B., "Shape optimisation of singly-symmetric cold-formed steel purlins", *Thin-Walled Structures*, **161**, 107402, 2021.

[24] Martins A. D., Camotim D., and Dinis P. B., "Distortional-global interaction in lipped channel and zed-section beams: Strength, relevance and DSM design", *Thin-Walled Structures*. **129**, 289-308, 2018.

[25] Martins A. D., Camotim D., and Dinis P. B., "On the distortional-global interaction in cold-formed steel columns: Relevance, post-buckling behaviour, strength and DSM design", *Journal of Constructional Steel Research*, **145**, 449-470, 2018.

[26] Talebian N., Gilbert B. P., Miller D., and Karampour H., "Biaxial bending design of solid steel storage rack uprights in global buckling", *Journal of Constructional Steel Research*, **196**, 107395, 2022.

[27] Schafer B. W., "Review: The direct strength method of cold-formed steel member design", *Journal of Constructional Steel Research*. **64**(7), 766-778, 2008.